HYBRID DWT WITH NARX NEURAL NETWORK FOR RESERVOIR INFLOW FORECASTING IN A CHANGING CLIMATE

THANNOB ARIBARG
College of Digital Innovation and Information Technology, Rangsit University, Pathum Thani, Thailand, thannob.a@rsu.ac.th

SEREE SUPHARATID
Climate Change and Disaster Center, Rangsit University, Pathum Thani, Thailand, seree.s@rsu.ac.th

ABSTRACT

Accurate and reliable long-term forecasting of reservoir inflow is necessary for efficient water resources' planning and management. In this study, a hybrid model using discrete wavelet transform (DWT) and the nonlinear autoregressive exogenous (NARX) neural network is developed for the simulation of the monthly inflow into Bhumibol and Sirikit reservoirs in Thailand under present and future climate scenarios. For this purpose, we have compiled an ensemble of nineteen downscaled climate data from NASA earth exchange global daily downscaled projections (NEX-GDDP). Two climate scenario projections (RCP 4.5 and RCP 8.5) are used to evaluate the climate change impacts for the future period up to 2099. Results indicate that climate change has a clear impact on both reservoirs inflow and show an increase in annual inflow into both reservoirs except in dry seasons. In the wet season (May-October), the inflow of Bhumibol and Sirikit reservoirs will increase by 6.61% and 17.41%, respectively, in the far future period (2079 - 2099) under RCP 8.5. Findings from this study imply how to adapt for the optimize water resource management in the future.

Keywords: climate change, discrete wavelet transform, nonlinear autoregressive exogenous neural network, RCPs, reservoir inflow

1. INTRODUCTION

The fifth Assessment Report (AR5) issued by the Intergovernmental Panel on Climate Change (IPCC) in 2013, described that the global average land and ocean surface temperature increased around the world by 0.85 °C from 1880 to 2012. The impact of climate change can lead to a change in water resources that reflected in temperature and precipitation. Precipitation is the most important source of water in a river, and it determines the amount of reservoir inflow.

To understand the impact of climate change on reservoir inflow, the global climate models (GCMs) are common tools for simulating climate. The framework of the fifth phase of the Coupled Model Intercomparison Project (CMIP5, Taylor et al., 2012) organized under the auspices of the World Climate Research Programme's (WCRP) Working Group on Coupled Modelling (WGCM), provides the largest set of climate model experiments to provide future projections and understand the past global climate change.

Neural networks (NN) are techniques that can estimate the nonlinear input and output relationship of complex systems characterized. In particular, NN is widely applied in reservoir inflow forecasting (Othman and Naseri, 2011; Vijayakumar and Vennila, 2016; Tiwari et al., 2013;). According to Valipour et al. (2013), nonlinear autoregressive neural network (NAR) indicated the best performance over static NN, autoregressive integrated moving average (ARIMA) and autoregressive moving average (ARMA) with regard to reservoir inflow forecasts in Iran. A nonlinear autoregressive exogenous (NARX) neural network has shown excellent performance over NN, NAR and nonlinear input-output (NIO) for forecasting the annual precipitation.

However, the NARX networks may not be able to cope up with the non-stationarity in input data. In order to relieve this problem, integration of discrete wavelet transform (DWT) techniques with the data-driven models has been developed for hydrological modeling. Emerging literature on DWT with NN has reported improvements in prediction accuracy (Kummong and Supratid, 2016).

The main objective of this study is to study the impact of climate change on reservoirs inflow over Chao Phraya River Basin in Thailand. The hybrid model of DWT and NARX was used with nineteen ensemble models form NASA earth exchange global daily downscaled projections (NEX-GDDP).

2. STUDY AREA AND DATA

2.1 Study area

Chao Phraya River Basin (CPRB) is located between longitude 98 - 101 °E and latitude 13.5 - 19 °N as shown in Fig. 1. The CPRB is the largest and most important river basin in Thailand, covering approximately 35 percent of the nation's land. Figure 1 shows the Chao Phraya River system. Four main sub rivers including the Ping, Wang, Yom, and Nan, merge at Nakhon Sawan (indicated by red star) to form the Chao Phraya River, which flows down to Bangkok (indicated by red rectangle) and discharging into the Gulf of Thailand. There are two large dam reservoirs exist in the basin. The Bhumibol has been operated since 1964 on the Ping River. The Sirikit reservoir, located on the Nan River. Both reservoirs, whose primary objectives are power generation and water resources.

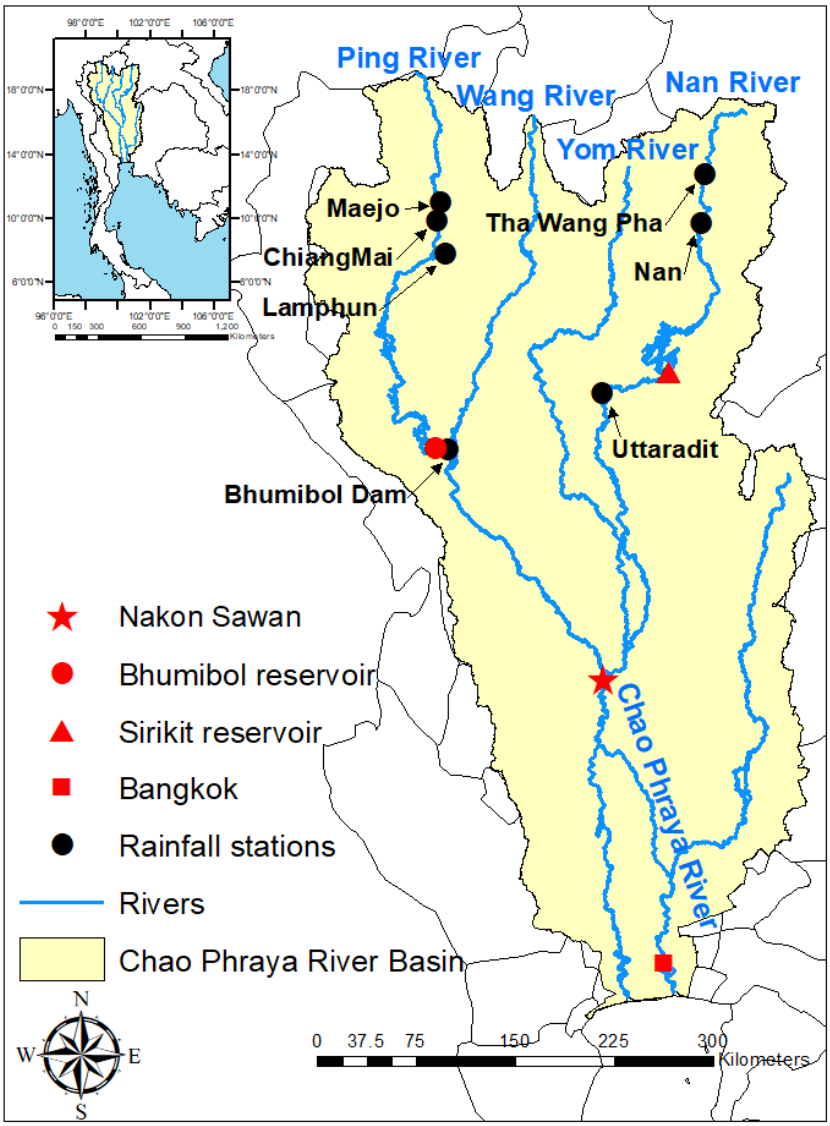

Figure 1. The Chao Phraya River Basin (yellow area) with Bhumibol (indicated by red circle) and Siriki reservoir (indicated by red triangle). The black dots mark the locations of rainfall stations.

2.2 Datasets

In this study we use nineteen statistically downscaled Global Climate Models (GCMs) from NASA Earth Exchange Global Daily Downscaled Projections (NEX-GDDP) (Thrasher et al., 2012). Then, the multi-model ensemble (MME) of monthly precipitation was downscaled to neighboring rainfall stations by using the distribution mapping (DM) (Teutschbein and Seibert, 2012). Two representative concentration pathways (RCPs) represent 'medium' (RCP 4.5) and 'high' (RCP8.5) scenarios featured by the radiative forcings of 4.5 and 8.5 W m^{-2} by 2100, respectively. Detailed information of the CMIP5 models was listed in Table 1. We have divided the future period from 2006 to 2099 into the near future (2010 to 2039), mid future (2040 to 2069) and far future (2070 to 2099).

Table 1. The CMIP5 models used in this study.

MODEL NAME	INSITUTION ID	CENTER AND COUNTRY	ORIGINAL RESOLUTION (LAT X LON)[A]	TYPE[B]
ACCESS1-0	CSIRO-BOM	Commonwealth Scientific and Industrial Research Organization and Bureau of Meteorology, Australia	1.25 × 1.875	AO
BCC-CSM1-1	BCC	Beijing Climate Center, China Meteorological Administration, China	2.8125 × 2.8125	ESM
BNU-ESM	GCESS	College of Global Change and Earth System Science, Beijing Normal University, China	2.8 × 2.8	ESM
CanESM2	CCCma	Canadian Center for Climate Modelling and Analysis, Canada	2.8 × 2.8	ESM
CCSM4	NCAR	National Center for Atmospheric Research, United States	0.9375 × 1.25	AO
CESM1-BGC	NSF-DOE-NCAR	Community Earth System Model Contributors	0.9 × 1.25	AO
CNRM-CM5	CNRM-CERFACS	Centre National de Recherches Météorologiques (CNRM), France	1.40625 × 1.40625	AO
CSIRO-Mk3-6-0	CSIRO-QCCE	Commonwealth Scientific and Industrial Research Organization in collaboration with Queensland Climate Change Centre of Excellence	1.850 × 1.875	AO
GFDL-ESM2G	NOAA/GFDL	NOAA/Geophysical Fluid Dynamics Laboratory, United States	2.0 × 2.5	ESM
GFDL-ESM2M			2.0 × 2.5	ESM
INM-CM4	INM	Institute for Numerical Mathematics	1.5 × 2.0	AO
IPSL-CM5A-LR	IPSL	Institut Pierre-Simon Laplace (IPSL), France	1.875 × 3.75	ChemESM
IPSL-CM5A-MR			1.25874 × 2.5	ChemESM
MIROC-ESM	MIROC	National Institute for Environmental Studies, The University of Tokyo, Japan	2.8125 × 2.8125	ChemESM
MIROC-EMS-CHEM	MIROC	National Institute for Environmental Studies, The University of Tokyo, Japan	2.8125 × 2.8125	AO
MRI-CGCM3	MRI	Meteorological Research Institute, Japan	1.125 × 1.125	ESM
MPI-ESM-LR	MPI-M	Max Planck Institute for Meteorology (MPI), Germany	1.875 × 1.875	ESM
MPI-ESM-MR	MPI-M	Max Planck Institute for Meteorology (MPI), Germany	1.875 × 1.875	AO
NorESM1-M	NCC	Norwegian Climate Centre, Norway	1.875 × 2.5	ESM

[A] All Models used are statistically downscaled to 0.25° resolution.

[B] AO :coupled atmospheric-ocean model; ESM :Earth system model; ChemESM :atmospheric chemistry coupled with ESM models.

3. METHODOLOGY

3.1 Nonlinear autoregressive exogenous (NARX) neural network

NARX network is another type of dynamic neural networks which are suitable for nonlinear dynamic systems and time series modeling and prediction. The defining mathematically equation for NARX network is shown in Eq. (1),

$$y(t) = f\big(y(t-1), y(t-2), \dots, y(t-d), u(t-1), u(t-2), \dots, u(t-d)\big) \quad (1)$$

where $y(t)$ and $u(t)$ are the input and output at time t, $y(t-1)$ is regressed on pervious values of the output at time t, d is time lag delay; The $f(\cdot)$ is a nonlinear function generated by NARX network. There are two different modes of NARX model, open-loop and close-loop as shown in Fig. 2. The open-loop calculates the future value of the target signal $y(t)$ from actual values of the input signal $u(t)$ and target output $y(t)$ during the NARX training phase. The close-loop calculates the output that is fed back from output to input.

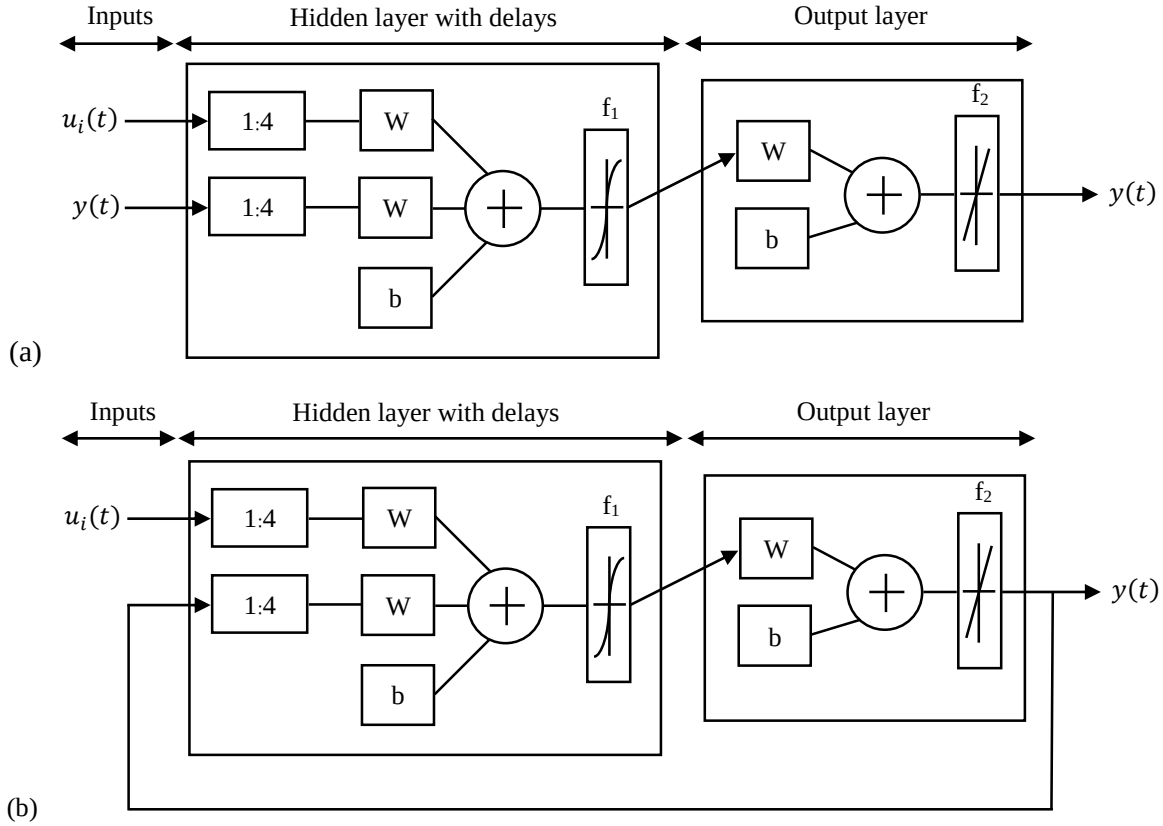

Figure 2. NARX network structure in open-loop (a) and closed-loop (b) with d = 4 delays.

3.2 Discrete wavelet transform (DWT)

DWT is developed based on Fourier transform. The DWT decomposes the original signal into low-frequency components and high-frequency components based on wavelet filtering basis functions as Eqs. (2) and (3).

$$L_l(t) = \sum_{\forall n} L_{l,n}\, \emptyset_{l,n}(t) \tag{2}$$

$$H_j(t) = \sum_{\forall n} H_{j,n} \psi_{j,n}(t) \tag{3}$$

where j = 1, 2, …, l are the levels of wavelet decomposition and n is a time interval. Function ϕ and ψ are called the low-pass and high-pass filtering basis function, respectively. Figure 3 represents the diagram of wavelet decomposition at level 3. Selection of suitable wavelet and the number of decomposition levels is very important in analysis of signals using the DWT.

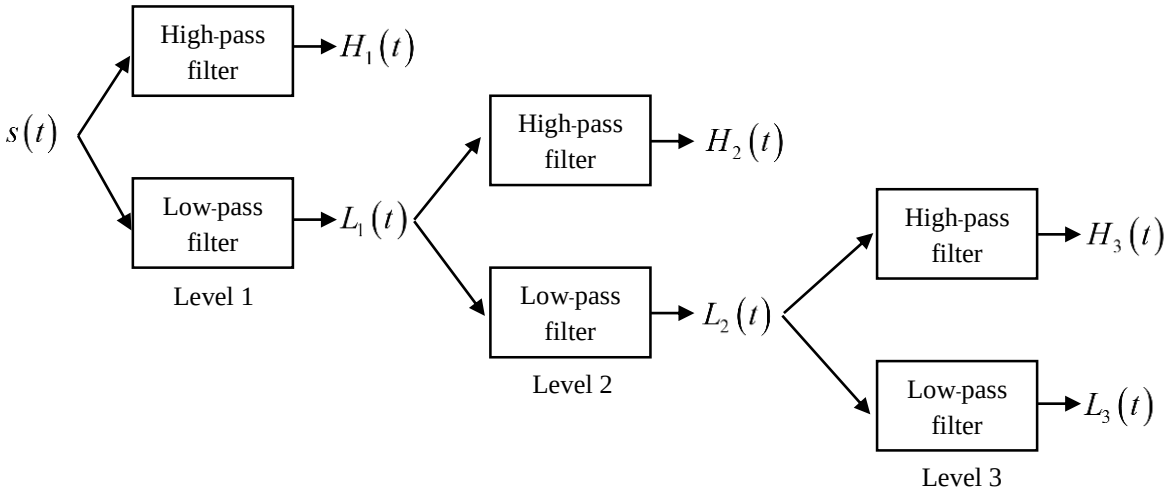

Figure 3. Diagram of wavelet decomposition at level 3.

From Fig. 3, the original signal $s(t)$ is broken down into two signals as an approximation (L_1) and detail (H_1) coefficients at level 1 by passing through low-pass and high-pass filters, respectively. The approximation is further decomposed and this process can be repeated to reach different resolution levels. The inverse discrete wavelet transform can be defined as Eq. (4) by reconstruction the original signal $s(t)$, using L_3, H_1, H_2, and H_3.

$$s(t) = H_l \sum_{j=1}^{l} H_j(t) \tag{4}$$

3.3 Hybrid model of DWT and NARX (DWT-NARX)

The proposed DWT-NARX approach is a hybrid of DWT and NARX neural network. To improve the modeling performance of standalone NARX, the reservoir inflows are estimated with the use of the climate change exogenous factors (MME monthly precipitation downscaled to near-by rainfall stations $i = 1,2,\dots,N$ from NEX-GDDP) which refers to $\boldsymbol{p}(t) = p_1(t), p_2(t), \dots, p_N(t)$; Figure 4 demonstrates a diagram of DWT-NARX for 3 level wavelet decomposition. The original time-series, $y(t)$ (which refers to reservoir inflow time-series) is decomposed into the coefficients of details, $H_1(t), H_2(t), \dots, H_l(t)$ (where l is decomposition level) and approximation, $L(t)$ sub-time series by using DWT. After decomposing, each sub-time series of both details and approximation and climate change exogenous input $\boldsymbol{p}(t)$ are imposed to an individual NARX using open-loop mode for model training purpose. All the output coefficients are supplied to inverse wavelet transform process for finally reconstructing the forecasted reservoir inflow. The procedure in the testing period is the same as the training period. For the future period, NARX with close-loop mode was used to perform the forecasted output.

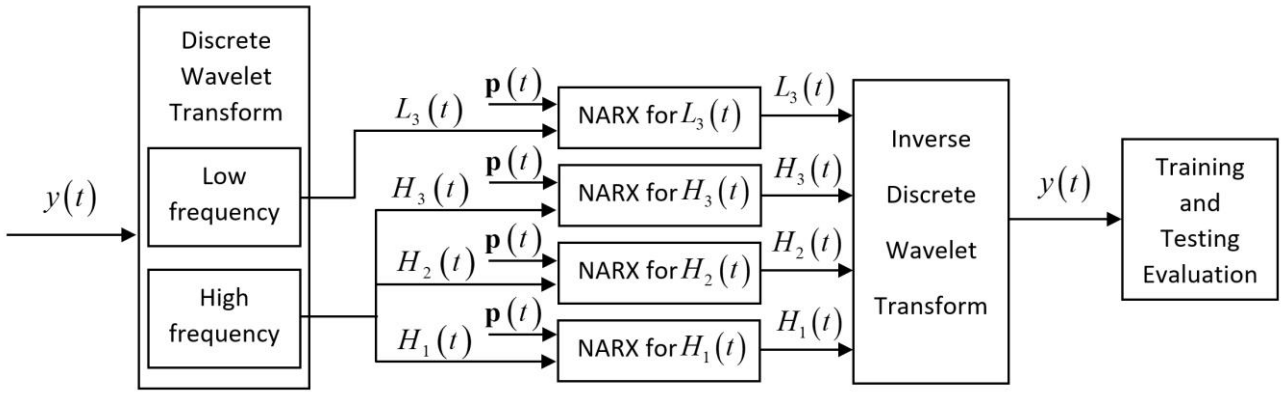

Figure 4. Diagram of DWT-NARX for a 3 level wavelet decomposition.

4. RESULTS

4.1 Performance of DWT-NARX for historical period

In this study, the DWT-NARX was used to forecast the mean monthly inflow of Bhumibol and Siriki reservoirs. The parameters of DWT-NARX were decided by several experimental runs. The comprehensive search of DWT-NARX parameters was done by varying the time delay from 2 to 4. The training and test periods were fixed from 1985 to 2005 and 1980 to 1984, respectively. The DWT-NARX was trained by the Levenberg-Marquard backpropagation method. Comparisons among other models (NARX, Elman's RNN, and BPNN) in the historical period reveal that the DWT-NARX perform the best performance in terms of Pearson's correlation coefficient (CC) and root mean square error (RMSE) as shown in Table 2.

Table 2. The performance measures in terms of CC and RMSE.

MODELS	BHUMIBOL RESERVOIR				SIRIKIT RESERVOIR			
	TRAINING		TESTING		TRAINING		TESTING	
	CC	RMSE	CC	RMSE	CC	RMSE	CC	RMSE
DWT-NARX	**0.9621**	**4.53**	**0.9180**	**9.59**	**0.9760**	**4.0309**	**0.9475**	**7.4467**
NARX	0.9566	23.46	0.6873	243.72	0.8303	107.59	0.7227	217.25
ELMEN'S RNN	0.8159	92.39	0.7647	112.74	0.6817	185.43	0.8416	129.62
BPNN	0.8356	83.00	-0.3429	928.90	0.6751	186.53	0.2170	989.90

4.2 Future inflow over Bhumibol and Siriki reservoirs

Figure 5 shows the annual inflow to Bhumibol and Siriki reservoirs of the observed data (black dash) and future inflows under RCP4.5 and RCP8.5. The maximum peak inflow increase 24% (329 mcm) in September and 14% (178 mcm) in August for Bhumibol and Siriki reservoirs, respectively.

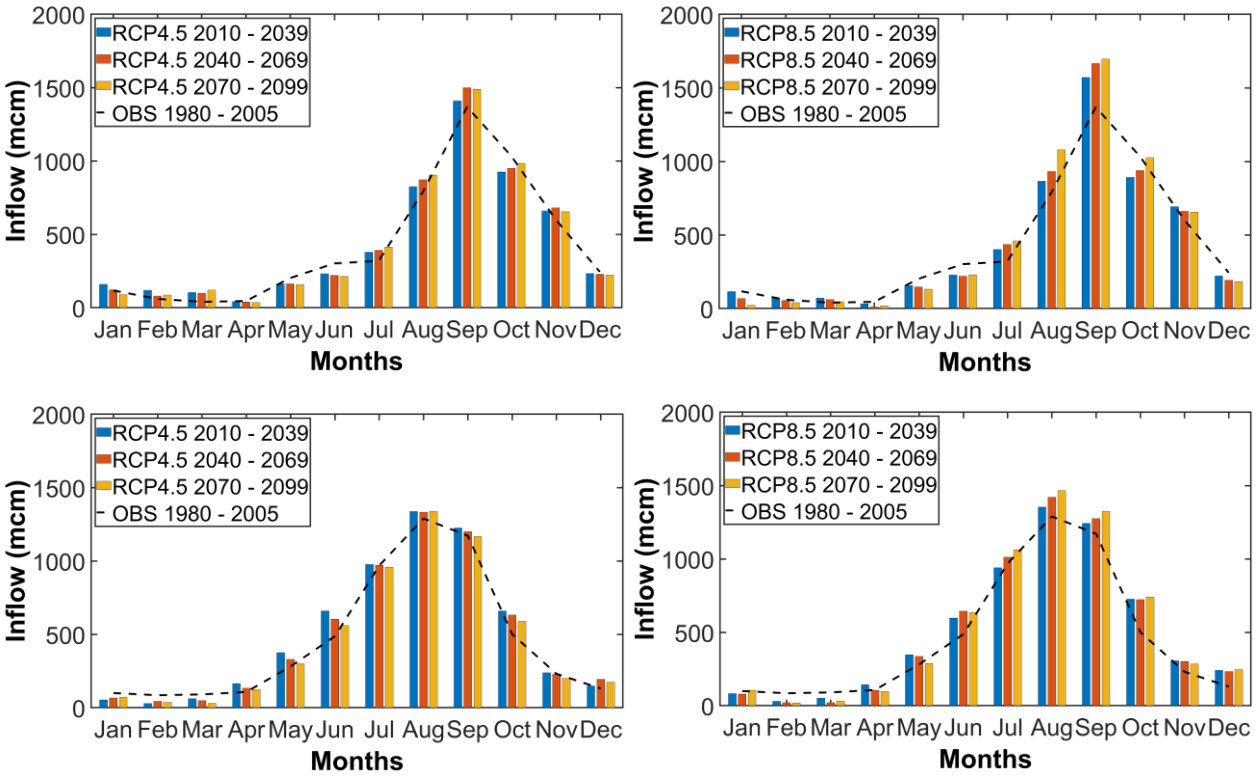

Figure 5. Annual inflow simulation to Bhumibol (a) and Sirikit (b) reservoirs under RCP4.5 and RCP8.5.

In addition, the change in the magnitude of future inflow for annual (Jan - Dec), wet (May - Oct), and dry (Feb - Apr) seasons was calculated comparison to the historical data. This was done only for RCP8.5 as shown in Fig. 6. Overall, there are agreements in increasing inflow for the annual and wet season. However, they show decreasing inflow in the dry season. On an annual scale, the inflow increases from 3.80% to 9.14% (Bhumibol) and 11.42% to 15.76% (Sirikit). In the wet season, the inflow to Bhumibol and Sirikit reservoirs will increase by 6.61% and 17.41%, respectively, in the far future period.

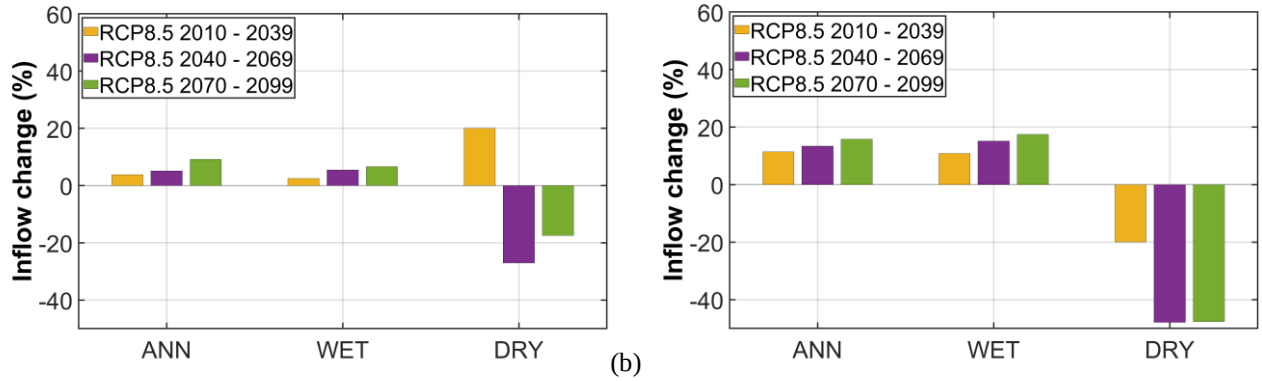

Figure 6. Change in magnitude of inflow for annual, wet, and dry to Bhumibol (a) and Sirikit (b) reservoirs with different future periods.

5. CONCLUSIONS

In this study, we investigate a hybrid model using discrete wavelet transform (DWT) and the nonlinear autoregressive exogenous (NARX) neural network, namely DWT-NARX, for forecasting the monthly inflow to Bhumibol and Sirikit reservoirs. We have compiled the multi-model ensemble (MME) of nineteen downscaled climate data from NASA earth exchange global daily downscaled projections (NEX-GDDP). Two climate scenario projections (RCP 4.5 and RCP 8.5) are used to evaluate the climate change impacts for the future period up to 2099. It was found that DWT-NARX shows the best performance in terms of Pearson's

correlation coefficient and root mean square error in the historical period. Then, we use DWT-NARX to forecast the future inflow. Overall, there are agreements in increasing inflow over the annual and wet season for both reservoirs. However, they show decreasing inflow in dry season. This finding will be useful to water resources policymakers in pondering whether the current drainage system is appropriate to meet the inflow changes in long-term periods.

ACKNOWLEDGMENTS

This work was financially supported by the Thailand Science Research and Innovation (TSRI) and the Thailand Office of Higher Education Commission (OHEC). We gratefully thank the Thai Meteorological Department (TMD) and Electricity Generating Authority of Thailand (EGAT) for providing the observed rainfall and reservoir inflow data, respectively. We also thank to the NASA Earth Exchange Global Daily Downscaled Projections (NEX-GDDP) from NASA Center for Climate Simulation (NCCS).

REFERENCES

Kummong, R., & Supratid, S. (2016). Thailand tourism forecasting based on a hybrid of discrete wavelet decomposition and NARX neural network. *Industrial Management & Data Systems*, 116(6):1242-1258.

Othman, F. and Naseri, M. (2011). Reservoir inflow forecasting using artificial neural network. *International journal of physical sciences*, 6(3): 434-440.

Valipour, M., Banihabib, M. E., and Behbahani, S. M. R. (2013). Comparison of the ARMA, ARIMA, and the autoregressive artificial neural network models in forecasting the monthly inflow of Dez dam reservoir. *Journal of hydrology*, 476:433-441.

Valipour, M. (2016). Optimization of neural networks for precipitation analysis in a humid region to detect drought and wet year alarms. Meteorological Applications, 23(1), 91-100.

Vijayakumar, N. and Vennila, S. (2016). Reservoir inflow forecasting at Krishnagiri Reservoir Project using artificial neural network. *In Proceedings of the National Conference on Contemporary Advancements in Civil Engineering Practices-CACEP*, PSG College of Technology, Coimbatore, India.

Taylor, K. E., Stouffer, R. J., and Meehl, G. A. (2012). An overview of CMIP5 and the experiment design. *Bulletin of the American Meteorological Society*, 93(4):485-498.

Teutschbein, C., & Seibert, J. (2012). Bias correction of regional climate model simulations for hydrological climate-change impact studies: Review and evaluation of different methods. *Journal of hydrology*, 456:12-29.

Tiwari, M. K., Song, K. Y., Chatterjee, C., and Gupta, M. M. (2013). Improving reliability of river flow forecasting using neural networks, wavelets and self-organising maps. *Journal of Hydroinformatics*, 15(2):486-502.